

Resonance Variations of the Microwave Refractive Index in YIG Plates

E. A. Kuznetsov^{a,b,*}, A. B. Rinkevich^a, and D. V. Perov^a

^a Mikheev Institute of Metals, Ural Branch, Russian Academy of Sciences, Yekaterinburg, 620012 Russia

^b Russian State Vocational Pedagogical University, Yekaterinburg, 620012 Russia

*e-mail: kuzeag@mail.ru

Received August 24, 2018; revised August 24, 2018; accepted November 19, 2018

Abstract—The influence of microwave resonance phenomena on complex refractive index in YIG plates has been theoretically and experimentally studied in the frequency range 26–38 GHz. It has been shown that a change in the magnetic field causes severe resonance-type changes in transmission and reflection factors. These changes are due both to effective interaction between millimeter electromagnetic waves and YIG plates (specifically, under ferromagnetic resonance conditions) and to the fulfillment of geometrical resonance conditions (when an integer number of half-waves or an integer odd number of quarter-waves are accommodated on the thickness of the plate). An algorithm to calculate complex refractive index with regard to the tensor-type magnetic permeability of YIG is suggested. The field and frequency dependences of complex refractive index have been analyzed. Geometrical resonance fields have been compared with extrema in the field dependences of the transmission and reflection factor moduli.

DOI: 10.1134/S1063784219050128

INTRODUCTION

Ferrites have found wide applications in microwave (1–110 GHz) devices, such as circulators, rectifiers, cavities, filters, and phase shifters, owing to a set of unique properties: high resistivity, high magnetic permeability, and high Curie temperature [1, 2].

Spinel ferrites were the first to be used in microwave engineering. At present, however, device designers give preference to garnet ferrites (specifically, yttrium ferrites and lanthanide ferrites) because of very low magnetic losses in them [3]. Garnets have a complex structure with general chemical formula $R_3Fe_5O_{12}$, where R stands for a trivalent rare-earth (Y, Gd, Tb, Dy, Ho, Er, Sm, or Eu) ion [4]. These materials are polycrystals and are produced using ceramic technology. Their important feature is a very small ferromagnetic resonance (FMR) linewidth [5]. It should be noted that when FMR linewidth ΔH is measured experimentally, the result strongly depends on the surface finish: the higher the surface finish, the smaller the FMR linewidth [6]. Although garnet ferrites have been studied for a long time owing to unique microwave properties, their potential has yet to be understood in full measure. Today, phenomena observed in thin YIG films (for example, spin-wave dark soliton pairs [7] and wideband dynamic chaos in an active ring oscillator [8]) are subjects of intense research.

However, systematic investigations of the YIG microwave refractive index have not been conducted

so far. The microwave refractive index can be determined by measuring the transmission and reflection coefficients of electromagnetic waves passing through and reflecting from a plate. Studies of microwave refractive index became still more important after it had turned out that this index may take anomalous (negative or near-zero) values under certain conditions [9]. Thus, it would be of much interest to trace the variation of microwave transmission and reflection coefficients under the action of a permanent magnetic field and see how this variation influences the behavior of complex refractive index under FMR and geometrical resonance conditions (the latter case implies that an integer odd number of quarter-waves or an integer number of half-waves are accommodated on the thickness of a plate). It is expected that the combined action of these resonances may cause an extraordinary change in transmission and reflection coefficients.

OBJECTS OF RESEARCH

We studied two YIG $Y_3Fe_5O_{12}$ polycrystalline samples synthesized by the sol–gel method from yttrium nitrate, iron nitrate, and an aqueous solution of citric acid (Research Institute Ferrit-Domen, St. Petersburg, Russia). Sample 1 with a thickness of 1.1 mm had a smooth (polished) surface with a roughness of ~ 1 – 2 μm . Sample 2 had a rough surface with a peak-to-peak height of about 100 μm and was 2 mm thick.

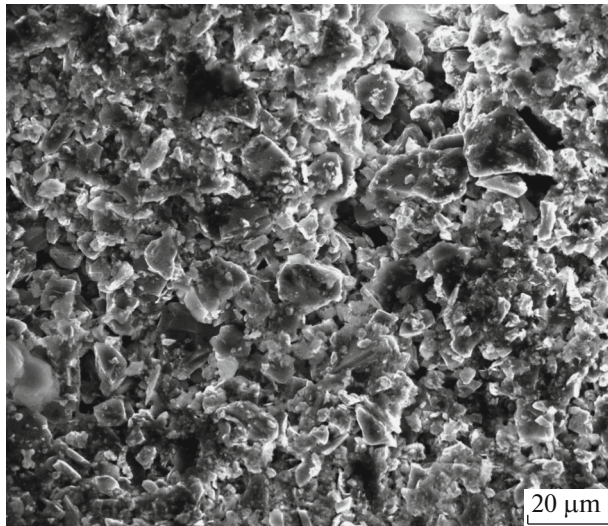


Fig. 1. Micrograph of 1.1-mm-thick sample 1.

The microstructures of the samples were examined in the Common Use Center at the Institute of Metals (Ural Branch, Russian Academy of Sciences) under a Quanta 200 scanning electron microscope with an accelerating voltage of 30 kV. The microscope was equipped with a Pegasus system allowing for electron backscatter diffraction (EBSD) studies. The microstructure of sample 1 obtained in the EBSD mode with $2000\times$ magnification is shown in Fig. 1. The grain size is within 8–10 μm . The chemical composition of samples was determined using energy-dispersive X-ray analysis. The composition of sample 1 was the following: O, 54.6%; Fe, 29.3%; Y, 16.1%. The composition of sample 2 was nearly the same: O, 53.8%; Fe, 27.3%; Y, 18.9%. These results are in fairly good agreement with the rated chemical composition of $\text{Y}_3\text{Fe}_5\text{O}_{12}$: O, 60%; Fe, 25%; Y, 15%.

MICROWAVE MEASUREMENTS AND RESULTS

Measurements were made in the frequency band 26–38 GHz by a method described elsewhere [10]. A sample was placed in the cross section of a rectangular waveguide and completely covered it. The cross-sectional area of the waveguide operating at the fundamental H_{10} mode measured 7.2×3.4 mm. Direct and backward waves were separated by means of directional couplers. The magnetic field dependence of the magnitudes of transmission coefficient D and reflection coefficient R was taken using a scalar network analyzer. Their relative variations were defined as $d_m = [|D(H)| - |D(0)|]/|D(0)|$, where $|D(H)|$ is the magnitude of the transmission coefficient in permanent magnetic field H and $r_m = [|R(H)| - |R(0)|]/|R(0)|$, where $|R(H)|$ is the magnitude of the reflection coefficient in permanent magnetic field H . Field H lies in the YIG

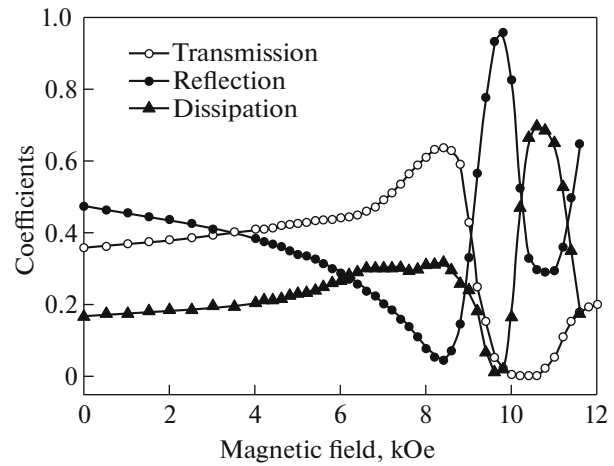


Fig. 2. Passage of microwaves through the YIG plate of sample 2: magnetic field dependences of transmission, reflection, and dissipation coefficients at 29 GHz.

plate's plane and is directed normally to microwave magnetic field H , $H \perp H_0$. All microwave measurements were made at room temperature.

Relative changes d_m and r_m in transmission and reflection coefficients measured in a magnetic field turned out to be anomalously high: up to 950%. Figure 2 plots the field dependences of transmission, reflection, and dissipation coefficients for sample 2 at 29 GHz. Dissipation Δ is calculated from measure coefficients D and R as

$$\Delta = 1 - |D|^2 - |R|^2.$$

Parameter Δ is the fraction of power that was absorbed and dissipated in a sample. When the magnetic field rises from 0 to 8.4 kOe, the reflection coefficient drops to a minimum of 0.046 and the transmission coefficient reaches a maximum of 0.637. The local maximum of dissipation is 0.317. Within 9.6–9.8 kOe, the dissipation, as well as the transmission coefficient, becomes minimal, $\Delta = 0.013$ and $D = 0.054$, whereas the reflection coefficient reaches a maximum, $R = 0.958$. Finally, in field interval 10.4–10.8 kOe, dissipation reaches a maximum of 0.697, the transmission coefficient drops to a minimum of 0.003, and the reflection coefficient exhibits a local minimum of 0.290. In this interval, FMR conditions are fulfilled. Thus, in field interval 0–12 kOe, the reflection, dissipation, and transmission coefficients change by 21, 52, and about 240 times, respectively.

DISCUSSION

The complex refractive index was calculated using two material parameters: dielectric permittivity ϵ and effective dynamic magnetic permeability μ_{eff} . It is given by

$$n = n' - in'' = \sqrt{\epsilon\mu_{\text{eff}}}, \quad (1)$$

where n' is the refractive index and n'' is the absorption coefficient.

Complex permittivity ϵ was found using an algorithm for its reconstruction. It is based on calculating the difference between the theoretical and experimental frequency dependences of the magnitudes of transmission and reflection coefficients [10]. This difference was then minimized by the least-squares method. It was found that real part ϵ' of complex permittivity ϵ equals 10.8 and the magnitude of its imaginary part ϵ'' is much smaller ($\epsilon'' \ll \epsilon'$). Hereinafter, it is assumed that ϵ' is constant and independent of magnetic field.

The magnetic permeability of YIG placed in a magnetic field is a tensor quantity. Under our experimental conditions, wavevector \mathbf{q} was normal to permanent magnetic field vector \mathbf{H}_0 and plane of the YIG plate, $\mathbf{q} \perp \mathbf{H}_0$, and effective magnetic permeability μ_{eff} can be expressed through the components of the dynamic permeability tensor [5]:

$$\mu_{\text{eff}} = \mu - \frac{\mu_a^2}{\mu}. \quad (2)$$

Here, μ and μ_a are diagonal and off-diagonal components of the magnetic permeability tensor.

The effective magnetic permeability can be found from the frequency and magnetic field dependences of μ and μ_a expressed in explicit form. To this end, it suffices to assume that these dependences have a standard Lorentz form.

Next, let us use the following expression for the dynamic magnetic permeability tensor [5]:

$$\bar{\mu} = \begin{pmatrix} \mu & i\mu_a & 0 \\ -i\mu_a & \mu & 0 \\ 0 & 0 & \mu_{\parallel} \end{pmatrix}, \quad (3)$$

where $\mu = 1 + 4\pi\chi$, $\mu_a = 4\pi\chi_a$, and $\mu_{\parallel} = 1 + 4\pi\chi_{\parallel}$. Here, dynamic magnetic permeability is expressed as

$$\chi = \frac{\chi' - i\chi''}{L} = \gamma M_0 \frac{\omega_H[\omega_H^2 - (1 - \alpha^2)\omega^2] - i\alpha\omega[\omega_H^2 + (1 + \alpha^2)\omega^2]}{L}, \quad (4a)$$

$$\chi_a = \frac{\chi'_a - i\chi''_a}{L} = \gamma M_0 \omega \frac{[\omega_H^2 - (1 + \alpha^2)\omega^2] - i2\alpha\omega\omega_H}{L}, \quad (4b)$$

$$\chi_{\parallel} = -\frac{i\alpha\gamma M_0}{\omega - i\alpha\omega_H}, \quad (4c)$$

where $L = [\omega_H^2 - (1 + \alpha^2)\omega^2]^2 + 4\alpha^2\omega^2\omega_H^2$, $\gamma = (g|e|)/(2mc)$ is the gyromagnetic ratio, g is the spectroscopic splitting factor, e is the electron charge, m is the effective electron mass, c is the propagation rate of an electromagnetic wave in vacuum, $\omega_H = \gamma H_0$, α is a

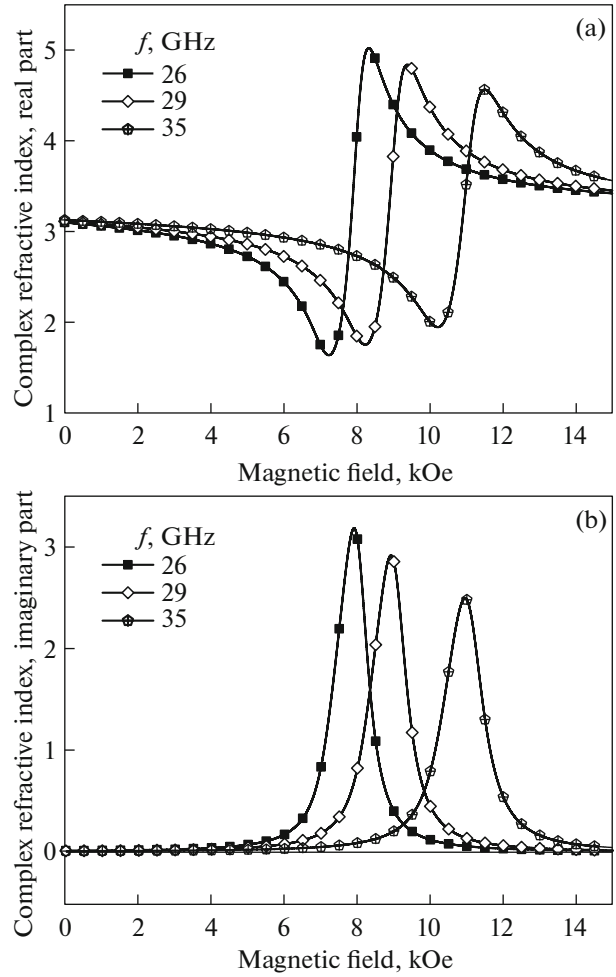


Fig. 3. Magnetic field dependences of microwave refractive index for sample 2: (a) real part and (b) imaginary part.

dimensional parameter in the Landau–Lifshitz–Gilbert equation, and M_0 is the saturation magnetization [5]. FMR linewidth ΔH was determined experimentally. For $\text{Y}_3\text{Fe}_5\text{O}_{12}$ garnet, saturation magnetization $4\pi M_0 = 1750$ G. Landau–Lifshitz–Gilbert parameter α was found from the width of the dissipation coefficient peak and turned out to be 0.043 for sample 2 and 0.01 for sample 1.

Figures 3 and 4 plot the field dependences of complex refractive index n , and Fig. 5 demonstrates the field dependences of effective magnetic permeability μ_{eff} . The dependences of the real parts of the refractive index are seen to be resonance curves, which shift along the abscissa axis toward higher fields with increasing frequency. The dependences of the imaginary parts of the refractive index exhibit resonance maxima. Certainly, the above resonance dependences of the refractive index result from a change in the dynamic magnetic permeability under FMR conditions. As has already been noted, test samples differ not only by thickness but also by surface conditioning;

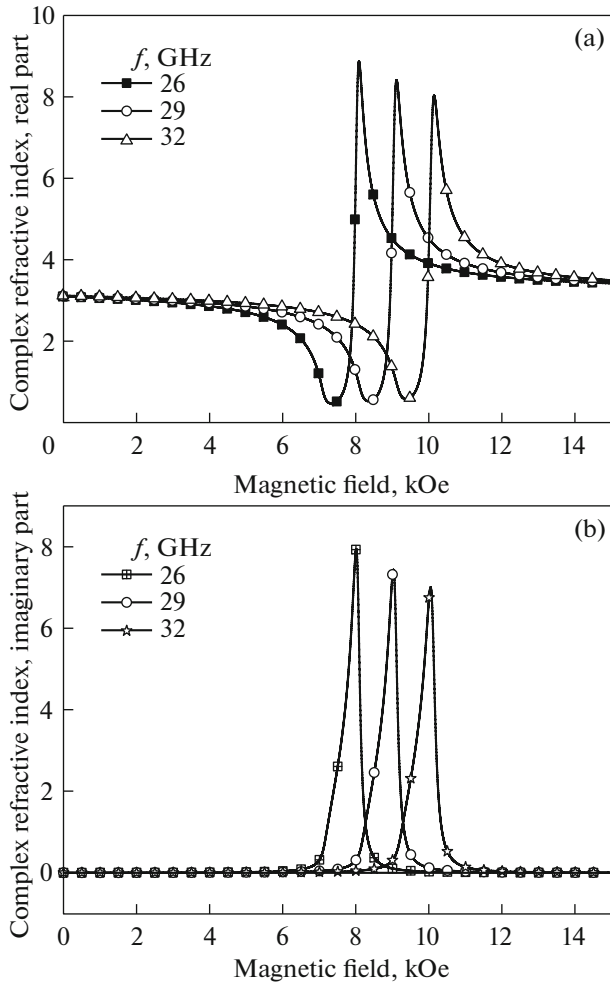


Fig. 4. Magnetic field dependences of microwave refractive index for sample 1: (a) real part and (b) imaginary part.

therefore, the peak of the imaginary part of the effective magnetic permeability (and, accordingly, of the refractive index) for sample 1 is narrower and the peak itself is higher. The real parts of n and μ_{eff} for sample 1 vary more strongly as well.

Of great interest is the fact that in fields below the FMR field, the real part of complex refractive index for sample 1 becomes less than unity, $n' < 1$. This value of refractive index results from strong variations of μ_{eff} . The question arises as to whether YIG becomes similar to the so-called epsilon-near-zero (ENZ) material [11] when condition $n' < 1$ is fulfilled? In both cases, the real part of the refractive index is positive but is less than unity. Such an unusual value of refractive index in ENZ materials is associated with a small real part of dielectric permittivity. In our case, the permittivity is high, $|\epsilon'| \gg 1$, and the “strange” value of n' is due to strong variations of the magnetic permeability, what is more, under conditions of strong absorption. Because of strong absorption, there is no direct analogy between our case and ENZ materials in contrast to

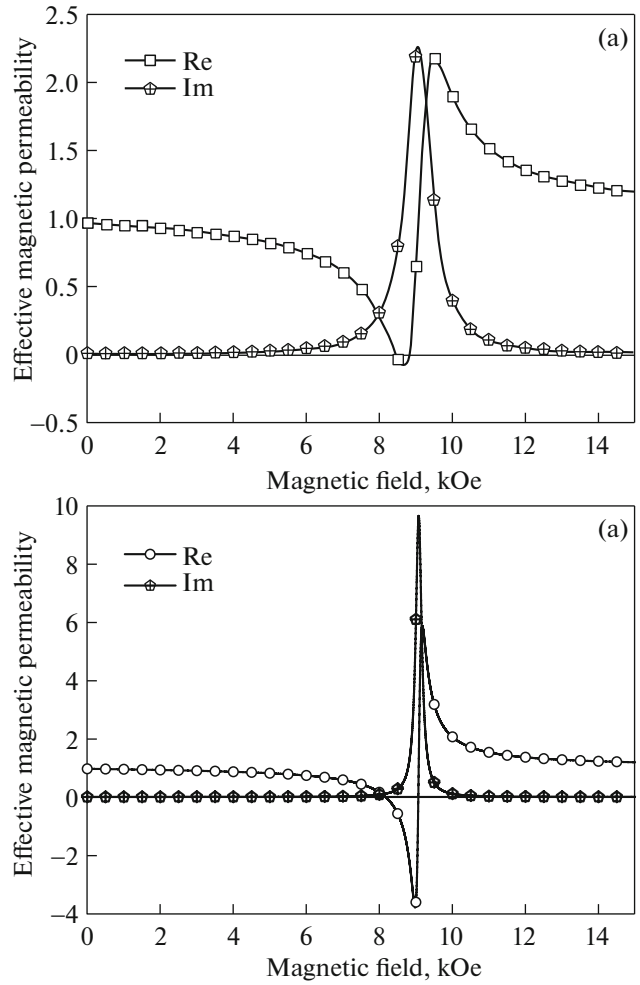


Fig. 5. Magnetic field dependences of complex effective magnetic permeability at 29 GHz for (a) sample 2 and (b) sample 1.

[12]. It should be noted that in our case it is unlikely that the real part of the refractive index can be made negative ($n' < 0$) through parameter variation. Indeed, the refractive index becomes negative if the real parts of both material constants, dielectric permittivity and magnetic permeability, are negative, as in double left-handed media [9]. In our case, permittivity is positive.

Figure 6 plots the frequency dependences of n taken at different fields. It is seen that these curves are nonmonotonic. The nonmonotonic variation of transmission and reflection coefficients can be explained by (i) effective interaction between millimeter electromagnetic waves and YIG plates, especially under FMR conditions, and (ii) fulfillment of the geometrical resonance condition (which implies that an integer number of half-waves or an integer odd number of quarter-waves are accommodated on the thickness of an YIG plate). Geometrical resonances lead to the appearance of standing waves in the plate.

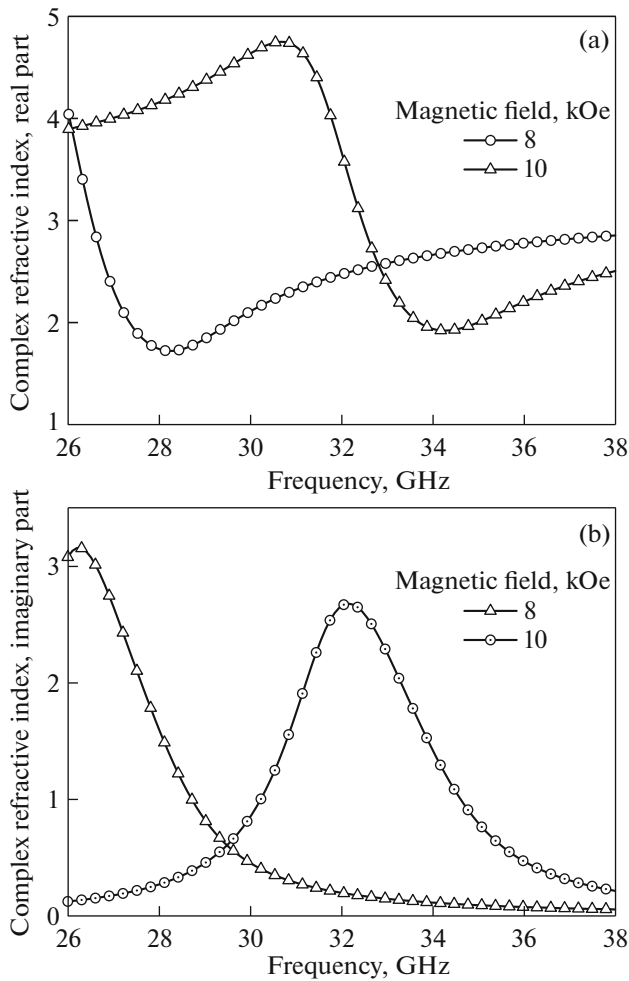


Fig. 6. Frequency dependences of complex refractive index in fields of 8 and 10 kOe for sample 2: (a) real part and (b) imaginary part.

Let us trace the behavior of these coefficients for sample 2 (Figs. 7a, 7b). Qualitatively, the experimental and theoretical curves are similar to each other. However, quantitatively they differ because of the difference between calculated (theoretical) and measured (experimental) FMR fields. The difference between the fields may be due to the porosity and demagnetization factor of the sample. The positions of geometrical resonances, when $d = \lambda/2$ and $d = 3\lambda/4$, are shown in Figs. 7a and 7b. By quantity λ is meant the length of an electromagnetic wave in a waveguide at given values of frequency and magnetic field strength. Two fields in which resonance condition $d = \lambda/2$ is fulfilled result from the nonmonotonic variation of real part μ' of the complex magnetic permeability (Fig. 5a).

The maximum of transmission coefficient D and the minimum of reflection coefficient R near field $H = 6.2$ kOe are related to geometrical resonance $d = \lambda/2$. With this condition met, the absolute value of the

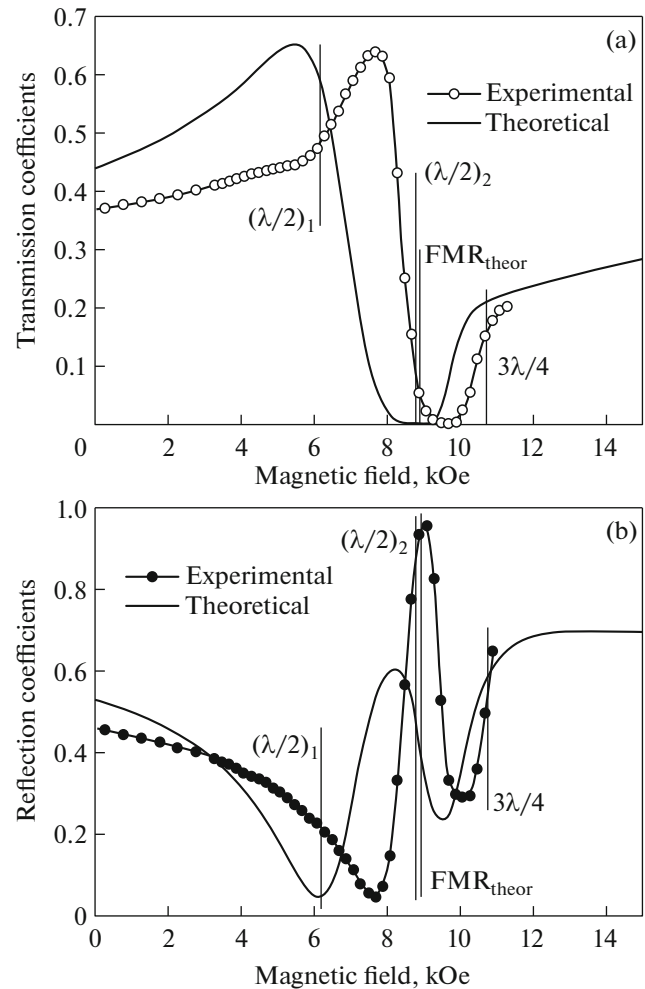


Fig. 7. Passage of microwaves through the YIG plate of sample 2: experimental vs. theoretical magnetic field dependences of (a) transmission and (b) reflection coefficients at 29 GHz. Theoretical values of the geometrical resonance and FMR fields are indicated.

ratio between the input impedances of the waveguide and YIG plate is $\xi = |Z_{in1}/Z_{in2}| \approx 1.54$.

At $H \approx 8.8$ kOe, resonance condition $d = \lambda/2$ is met again. When this condition is met, the transmission coefficient is usually high [13]. However, the impedance ratio in our case is high, $\xi \approx 3.76$, because of the nonmonotonic variation of μ' and reflection coefficient becomes large, $R \approx 0.48$ (transmission and reflection coefficients obtained under geometrical resonance conditions are compared with the calculated curve).

In the FMR range at $H \approx 9.1$ kOe, D and R reach a maximum because of strong absorption. These data are again compared with the calculated curve. It is seen in Fig. 5a that μ''_{eff} is maximal at this field as well.

In field $H \approx 10.8$ kOe, condition $d = 3\lambda/4$ is fulfilled. With this condition met, the reflection coefficient is usually minimal [13]. In our case, when the

effective magnetic permeability varies, the input impedance ratio is high, $\xi \approx 8-8.75$. It is therefore not surprising that the reflection coefficient is large, $R \approx 0.6-0.7$.

CONCLUSIONS

The influence of microwave resonance phenomena on the complex refractive index of two YIG ($Y_3Fe_5O_{12}$) plates was studied theoretically and experimentally in the frequency range 26–38 GHz.

An algorithm to calculate the complex refractive index n was developed for the case of an electromagnetic wave incident on the surface of a ferromagnetic dielectric placed in a permanent magnetic field with regard to tensor-type magnetic permeability.

The field and frequency dependences of the real and imaginary parts of the refractive index were analyzed. It was shown that great variations of reflection and transmission coefficients cause large variations of complex refractive index. Physical reasons for such large variations seem to be the fulfillment of ferromagnetic resonance conditions and conditions $d = \lambda/2$ and $d = 3\lambda/4$ for geometrical resonances.

FUNDING

This study was supported by the Russian Science Foundation (grant no. 17-12-01002 Refractive Index of Inhomogeneous Media in a Magnetic Field and Microwave Field Nonuniformity).

ACKNOWLEDGMENTS

Electron microscopic examinations were conducted in the Common Use Center (Institute of Metals, Ural Branch, Russian Academy of Sciences).

REFERENCES

1. Ü. Özgür, Y. Alivov, and H. Morkoc, *J. Mater. Sci.: Mater. Electron.* **20**, 789 (2009).
2. V. G. Harris, *IEEE Trans. Magn.* **48**, 1075 (2012).
3. M. I. Martynov, A. A. Nikitin, A. B. Ustinov, and B. A. Kalinikos, *Proc. All-Russian Conf. "Microwave Electronics and Microelectronics," St. Petersburg, Russia, 2015*, p. 130.
4. Yu. M. Yakovlev and S. Sh. Gendelev, *Ferrite Single Crystals in Radio Engineering*, Ed. by G. A. Matveev (Sovetskoe Radio, Moscow, 1975).
5. A. G. Gurevich and G. A. Melkov, *Magnetic Oscillations and Waves* (Fizmatlit, Moscow, 1994).
6. A. Ustinov, V. Kochemasov, and E. Khas'yanova, *Elektronika*, No. 8, 86 (2015).
7. Z. Wang, M. Cherkasskii, B. A. Kalinikos, and M. Wu, *Phys. Rev. B* **91**, 174418 (2015).
8. A. Kondrashov, A. Ustinov, M. Cherkasskii, B. A. Kalinikos, and S. O. Demokritov, *Proc. 8th Joint European Magnetics Symp., Glasgow, United Kingdom, 2016*.
9. *Electromagnetic Metamaterials: Physics and Engineering Explorations*, Ed. by N. Engheta and R. W. Ziolkowski (Wiley, 2006).
10. A. B. Rinkevich, M. I. Samoilovich, S. M. Klescheva, D. V. Perov, A. M. Burkhanov, and E. A. Kuznetsov, *IEEE Trans. Nanotechnol.* **13**, 3 (2014).
11. M. G. Silveirinha and N. Engheta, *Phys. Rev. Lett.* **97**, 157403 (2006).
12. A. B. Rinkevich, D. V. Perov, M. I. Samoilovich, and S. M. Klescheva, *Metamaterials* **6**, 27 (2012).
13. L. M. Brekhovskikh, *Waves in Layered Media* (Akad. Nauk SSSR, Moscow, 1957).

Translated by V. Isaakyan